

Review

Padé Approximants, Their Properties, and Applications to Hydrodynamic Problems

Igor Andrianov ^{1,*} and Anatoly Shatrov ^{2,3}

¹ Chair and Institute of General Mechanics, RWTH Aachen University, Eilfschornsteinstraße 18, D-52062 Aachen, Germany

² Institute of Mathematics and Information Systems, Vyatka State University, Moskovskaya 36, RU-610000 Kirov, Russia; shatrov@vyatsu.ru

³ Department of Physics and Medical Informatics, Kirov State Medical University, Karl Marx 112, RU-610000 Kirov, Russia

* Correspondence: igor.andrianov@gmail.com

Abstract: This paper is devoted to an overview of the basic properties of the Padé transformation and its generalizations. The merits and limitations of the described approaches are discussed. Particular attention is paid to the application of Padé approximants in the mechanics of liquids and gases. One of the disadvantages of asymptotic methods is that the standard ansatz in the form of a power series in some parameter usually does not reflect the symmetry of the original problem. The search for asymptotic ansatzes that adequately take into account this symmetry has become one of the most important problems of asymptotic analysis. The most developed technique from this point of view is the Padé approximation.

Keywords: Padé approximants; multi-point Padé approximants; perturbation method; matching; boundary layer; rotating fluid; Ekman layer



Citation: Andrianov, I.; Shatrov, A. Padé Approximants, Their Properties, and Applications to Hydrodynamic Problems. *Symmetry* **2021**, *13*, 1869. <https://doi.org/10.3390/sym13101869>

Academic Editor: Iver H. Brevik

Received: 6 August 2021

Accepted: 18 September 2021

Published: 4 October 2021

Publisher's Note: MDPI stays neutral with regard to jurisdictional claims in published maps and institutional affiliations.



Copyright: © 2021 by the authors. Licensee MDPI, Basel, Switzerland. This article is an open access article distributed under the terms and conditions of the Creative Commons Attribution (CC BY) license (<https://creativecommons.org/licenses/by/4.0/>).

1. Introduction

“Taylor series per se are almost useless. The real power of power series is in combination with other ideas. . . . Power series in isolation are almost never useful to solve boundary-value problems because it is only occasionally that the radius of convergence is sufficiently large to embrace both boundaries. Nevertheless, when combined with another idea, Padé approximants (PAs), power series become an effective tool for ordinary differential equation boundary-value problems” [1].

The use of PAs allows us in many cases to overcome the local nature of the obtained solutions inherent in the methods of series and the method of perturbations [1–6].

In this paper, we first provide an overview of PAs, and then describe the advantages of using PAs for solving specific hydrodynamic problems.

Problems of the flow of incompressible viscous liquid in rotating channels are considered. More exactly, we investigate thin domains near horizontal walls perpendicular to the axis of rotation. At high speeds of channel rotation, the so-called Ekman layers are formed in these domains. As a result, the flow region in the rotating channel is divided into boundary layers with an inhomogeneous distribution of velocity components and a core with a uniform velocity distribution.

The appearance of Ekman layers leads to the formation of two flows in the rotating channel. The main flow with a velocity w is formed in the direction of the Oz axis, and the secondary flow u is formed in the direction of the Ox axis.

In this paper, we also aim to study the structure of Ekman boundary layers by asymptotic methods using PAs.

This paper is organized as follows. We present the definition of PAs and describe their general properties in Section 2. Sections 3 and 4 describe the merits and drawbacks of

	n				
m		0	1	2	...
0		$f_{[0/0]}(\epsilon)$	$f_{[1/0]}(\epsilon)$	$f_{[2/0]}(\epsilon)$...
1		$f_{[0/1]}(\epsilon)$	$f_{[1/1]}(\epsilon)$	$f_{[2/1]}(\epsilon)$...
2		$f_{[0/2]}(\epsilon)$	$f_{[1/2]}(\epsilon)$	$f_{[2/2]}(\epsilon)$...
...	

The terms of the first row of the Padé table correspond to the finite sums of the Maclaurin series. If the degrees of the numerator and the denominator are equal ($n = m$), one obtains the diagonal PA, the most common in practice. Note that the Padé table may contain gaps for those indices n, m for which a PA does not exist.

The continued fractions [9] method is similar to the PA method. There are several types of continued fractions. A regular C-fraction is an infinite sequence, the first N terms of which are of the form

$$f_N(\epsilon) = a + \frac{c_0}{1 + \frac{c_1 \epsilon}{1 + \frac{c_2 \epsilon}{\dots + \frac{c_{N-1} \epsilon}{1 + c_N \epsilon}}}} \tag{8}$$

The coefficients c_i are obtained after the expansion of expression (8) in the Maclaurin series, followed by equating the coefficients at the same powers of ϵ . At $a = 0$, one obtains Stieltjes continued fractions or an S-fraction. For the Stieltjes function

$$S(\epsilon) = \int_0^\infty \frac{\exp(-t)}{1 + \epsilon t} dt$$

the expansion coefficients (8) have the form: $a = 0, c_0 = 1, c_{2n-1} = c_{2n} = n, n \geq 1$.

For a description of different types of continued fractions, algorithms for their construction, and application areas, see [9]. The advantage of continued fractions is the significant reduction in the number of “long” arithmetic operations (multiplications and divisions).

Many methods, such as the Aitken, Shanks, eta, and epsilon methods, are mathematically equivalent to the evaluation of certain Padé approximants but have traditionally been formulated algorithmically by fast recurrence relations related to continued fractions in the interests of speed [10,11].

Let us note some properties of PAs [6]:

1. If a PA exists for the chosen m and n , it is unique.
2. If the sequence PA converges to a given function, the roots of its denominator tend to the poles of the function.
3. A PA realizes a meromorphic continuation of a function given by a power series.
4. The PA of the inverse function is equal to the PA inversion of the function itself. This property is called duality and is more strictly formulated as follows. If $q(\epsilon) = f^{-1}(\epsilon)$ and $f(0) \neq 0$, then

$$q_{[n/m]}(\epsilon) = f_{[n/m]}^{-1}(\epsilon)$$

provided that one of these approximations exists.

5. Diagonal PAs are invariant under linear fractional transformations of the argument. Let the function be given by its expansion (1). Consider a linear fractional transformation $W = a\epsilon / (1 + b\epsilon)$ that preserves the origin and a function $q(W) = f(\epsilon)$. Then

$$q_{[n/n]}(W) = f_{[n/n]}(\epsilon) \tag{9}$$

provided that one of these approximations exists.

- 6. Diagonal PAs are invariant under linear fractional transformations of functions. Let function (1) be given. We put

$$q(\varepsilon) = \frac{a + bf(\varepsilon)}{c + df(\varepsilon)}$$

If $c + df(0) \neq 0$, then

$$q_{[n/n]}(\varepsilon) = \frac{a + bf_{[n/n]}(\varepsilon)}{c + df_{[n/n]}(\varepsilon)} \tag{10}$$

provided that $f_{[n/n]}(\varepsilon)$ exists. Due to this property, infinite PA values can be considered to be on par with finite ones.

- 7. PAs allow us to obtain upper and lower bounds on the values of a function. The diagonal PA gives the estimates

$$f_{[n/n-1]}(\varepsilon) \leq f_{[n/n]}(\varepsilon) \leq f_{[n/n+1]}(\varepsilon) \tag{11}$$

As a rule, this estimate is also true for the function itself, i.e., $f_{[n/n]}(\varepsilon)$ in expression (9) can be replaced by $f(\varepsilon)$.

3. Merits and Drawbacks of PAs

The mathematical theory of PAs has been developed quite deeply [6,11,12]. However, rigorous mathematical theorems are focused on the widest possible classes of functions, including those that are pathological from the point of view of practical applications. Therefore, the general assessments obtained along this path are often too pessimistic. For example, the very general theorem of Gonchar [12] states: if none of the diagonal PAs $f_{[n/n]}(\varepsilon)$ has poles in a circle of radius R , then the sequence $f_{[n/n]}(\varepsilon)$ converges uniformly in this circle to the original function $f(\varepsilon)$. Moreover, the absence of poles of the sequence $f_{[n/n]}(\varepsilon)$ in a circle of radius R implies the convergence of the original Taylor series in this circle. Since the diagonal PAs are invariant under linear fractional maps $\varepsilon \rightarrow \frac{\varepsilon}{(a\varepsilon + b)}$, the theorem is true for any open circle containing a decomposition point and for any domain that is the union of these circles. A significant drawback for practice is the need to check all diagonal PAs. If in a disc of radius R only some sequence of diagonal PAs has no poles, then its uniform convergence to the original function holomorphic in the given disc is guaranteed only for $R < R_0$, where $0.583R < R_0 < 0.584R$ [13].

For practical applications, the most acceptable means of studying PA properties are numerical experiments. In particular, on their basis, it can be argued with a high degree of reliability that in the overwhelming majority of practically important cases $R \gg R_0$.

The epsilon method, as shown in [14], is the most promising from the point of view of summing diverging or poorly converging series.

As a rule, the rate of convergence of rational approximations significantly exceeds the rate of convergence of polynomial approximations. For example, the function e^z in the circle of convergence is approximated by a diagonal PA of the n -th degree $4n$ times better than by an algebraic polynomial of degree $2n$. This is even more noticeable for functions of limited smoothness. E.g., the function $|\varepsilon|$ on the interval $[-1, 1]$ cannot be approximated by an algebraic n -polynomial so that the order of approximation is better than $1/n$. The PA gives the rate of convergence $\sim \exp(-\sqrt{2n})$ [15].

As a result of numerical experiments, it was found that diagonal and close to diagonal PA sequences often have the autocorrection property [16–19]. Its essence is as follows. To determine the coefficients of the numerator and denominator, one has to solve systems of linear algebraic equations. This is an ill-posed operation, so the PA coefficients will be determined with large errors. However, these errors are in a sense self-compensated; therefore, the PA's approximation of the original function is high. This is the radical

difference between PA and the Taylor series, in the calculation of which the error only grows with an increase in the number of terms.

The occurrence of the autocorrection property has been numerically tested for a number of special functions. At the same time, for elliptic functions, the so-called spurious pole-zero pairs or “Froissart doublets” appear, formed by closely spaced (but different and irreducible) zeros and PA poles. This suggests that the PA in the general case is ill-posed. The reason the PA is ill-posed is that it is related to an analytic continuation, since the aim is typically to gain information about a function in a region of the complex plane based on information at a single point [8].

4. Generalizations of the PA

Among the methods for removing doublets, one can be mentioned that is based on explicit computation of zeros and poles [20,21].

For eliminating spurious poles, in [22] the smoothed PA was proposed. Its essence is to use the averaged (in a certain sense) expression instead of the usual diagonal PA $p_n(\epsilon)/q_n(\epsilon)$:

$$f_{[n/n]}(\epsilon) = \frac{q_n(\epsilon)p_n(\epsilon) + q_{n-1}(\epsilon)p_{n-1}(\epsilon)}{q_n^2(\epsilon) + q_{n-1}^2(\epsilon)} \tag{12}$$

The authors of [23] propose another variant of a weighted average in which the spurious zero-pole pairs give a strongly reduced contribution.

The so-called robust PA [8] is based on slightly reducing the accuracy of the solution to a certain matrix problem; the benefit is that the resulting PAs will be pole-free in most regions where the original function itself is pole-free.

The PA described above is sometimes called the PA of the first kind [5,24]. The PA of the second kind, or multipoint PA (MPA), is a rational function $f_{[n/m]}(\epsilon)$ of the form (2) such that its values for the $n + m + 1$ values of the argument coincide with the values of $f(\epsilon)$ at the same points. This gives a system of linear algebraic equations for determining the coefficients of the polynomials of the numerator and denominator [24]. The MPA in many cases provides effective interpolation formulas and allows for extrapolating the values of a function specified on a limited interval beyond its limits [25,26].

The PA allows you to successfully work with functions that have poles. However, it is often necessary to investigate functions that have branch points and build all their branches. In this case, Hermite-Padé [27] approximations can be used. Let it be a question of a function having the following expansion

$$f(\epsilon) = \sum_1^\infty u_n \epsilon^n, f_N(\epsilon) = \sum_1^N u_n \epsilon^n. \tag{13}$$

If function (11) has a branch point, then to search for branches, one can go to an implicit function and construct a polynomial $F_p(\epsilon, f)$ of degree $p \geq 2$

$$F_p(\epsilon, f) = \sum_{m=1}^p \sum_{k=0}^m C_{m-k,k} \epsilon^{m-k} f^k, C_{0,1} = 1 \tag{14}$$

whose coefficients are determined from the condition

$$F_p(\epsilon, f_N(\epsilon)) = O(\epsilon^{N+1}) \text{ at } \epsilon \rightarrow 0 \tag{15}$$

The polynomial F_p contains $0.5(p^2 + 3p - 2)$ unknowns and condition (12) yields N linear algebraic equations; therefore, there should be $N = 0.5(p^2 + 3p - 2)$.

After the polynomial F_p has been found, one can easily find the p branches of the solution to the equation

$$F_p = 0 \tag{16}$$

There also exist many other generalizations of the PA. E.g., the Padé–Fourier and Padé–Chebyshev approximants [7,11] use trigonometric functions or orthogonal polynomials. A PA in two variables is called a Chisholm approximant; a PA in multiple variables is called a Canterbury approximant [7].

5. Using PAs in Nonlinear Mechanics

Initially, PAs were applied in physics for the analysis of divergent and asymptotic series [5,6] and in the theory of critical phenomena. They are also widely used in the mechanics of solids, especially in such areas as wave dynamics (improving convergence, overcoming the Wilbraham–Gibbs phenomenon, and building concentrated nonlinear waves [3]), discrete lattices theory (construction of improved continuous models), and the theory of composites [28].

It is worth noting the geometric series method for the construction of nonlinear concentrated waves [29–31]. In this approach, the solution is found in the form of a series in powers of the exponential function and, using the PA, the conditions under which the series becomes geometric are revealed.

Using PAs in asymptotic approaches with unconventional perturbation parameters [3,32] can greatly extend the range of applicability of perturbation series. Especially noteworthy is the method of the homotopy (“artificial small”) parameter, which made it possible to propose a new technique for solving mixed problems of mathematical physics [3]. Two- and multipoint PAs (the TPPA, the MPA) proved to be very effective tools for constructing global approximations from asymptotic expansions [2,3,25,26]. A natural generalization of this approach is the two-point quasifractional approximant method [26], which is also called the asymptotically equivalent functions method [2,3] or the asymptotic approximants approach [33].

6. Using PAs in Boundary Layer Problems

The pioneering papers by Van Dyke [34–36] are devoted to the application of PA in hydrodynamics. An overview of the work done in this area up to 1994 is contained in the monograph by Pozzi [37]. Since that time, PAs have taken their rightful place in the mechanics of liquids and gases [38,39]. The results obtained after 1994 are partially highlighted in our review [39]. In this section, we focus on applying PAs to boundary layer problems.

The history of the emergence and development of the concept of a boundary layer is described in detail in [40–42]. Recall that the key (for singular asymptotics) concept of an edge effect occurred in the works of H. Lamb and A.B. Basset in 1890, while the concept of a boundary layer occurred in fluid mechanics in 1904 [43]. An extremely interesting and useful visual illustration of this concept is the album of photographs of liquid and gas flows [44]. The works of Vishik and Lyusternik [45,46] played a significant role in the mathematical formulation of the boundary layer idea. They considered boundary layers for ODEs and linear and quasilinear PDEs of elliptic and parabolic type. The initial layers [47,48] were also studied.

In various fields of science, the terms ‘stiff equation’, ‘contrast structure’, ‘edge effect’, and ‘skin effect’ are used to describe the phenomena of the boundary layer. In any case, such an asymptotic phenomenon is based on the principle of spatial or temporal localization [49].

Before the computer revolution, methods for solving boundary layer equations relied on phenomenological or asymptotic approaches. Kármán and Polgauzen [50,51] proposed that we limit ourselves to satisfying these equations only on average over the thickness of the boundary layer. For this purpose, one should use the momentum theorem and replace the differential equations with integral relations obtained from the equation of motion by integrating it over the thickness of the boundary layer.

The Kochin–Loitsyanskii [50,51] method uses the idea of an “intermediate” asymptotic. An arbitrary distribution of velocities on the outer boundary of the boundary layer is replaced by a linear distribution in the first approximation, a quadratic distribution in

the second, etc., representations that perform smooth matching with the solution in the main zone. Later, this idea was developed by Loitsyanskii in the method of “generalized similarity” [51].

The computer revolution has led to the creation of effective numerical methods for solving the boundary layer equations [52,53]. This devalued a number of phenomenological approaches, but only increased the role of asymptotic methods [54–56].

A feature of boundary layer problems is the nonuniformity of the asymptotic expansion. The boundary layer is the region of singularity, and its solution is called the inner asymptotic. The solution in the outer region is called the regular (outer) asymptotic. If the conditions of the Kaplun theorem [57] are satisfied, the regular asymptotic can be uniformly extended in such a way that an overlap region arises where it is possible to compare the inner and outer asymptotics. The method of matched asymptotic expansions [54,58] is based on this. However, it is not always easy to justify the applicability of the Kaplun theorem [57]. This implies the relevance of methods for the synthesis of various limiting asymptotics. Below, we consider the matching of inner and outer asymptotics using the PA. Let us consider as an example the laminar boundary layer near a flat plate [50] described by the Blasius equation

$$\phi''' + \phi\phi'' = 0 \quad (17)$$

with BCs

$$\phi(0) = \phi'(0) = 0 \quad (18)$$

$$\phi'(\infty) = 2 \quad (19)$$

where $\phi(\zeta) = \frac{\psi}{\sqrt{x}}$, $\psi(y)$ is the stream function, $\zeta = \frac{y}{2} \sqrt{\frac{Re}{x}}$ is the self-similar variable, x, y are the Cartesian coordinates, and the x -axis is plotted along the plate in the direction of the stream.

The inner asymptotic (17)–(19) ($\zeta \rightarrow 0$) is

$$\phi = a_2\zeta^2 - \frac{a_2^2}{30}\zeta^5 + O(\zeta^8) \quad (20)$$

The construction of the outer asymptotic is nontrivial due to the presence of logarithmic terms. In [38,39], the mechanism for obtaining and estimating both the main and minor terms of the outer asymptotic is described in detail. The expression for the outer asymptotic ($\zeta \rightarrow \infty$) has the form

$$\phi \sim 2\zeta - c + \frac{2a_2D}{(2\zeta - c)^2} \exp(-\zeta^2 + c\zeta) \quad (21)$$

The constants a_2, c, D are determined by the integral relations

$$D = \exp\left(-\int_0^\infty (\phi_a - 2\zeta + c) d\zeta\right) \quad (22)$$

$$a_2 = \frac{1}{2} \int_0^\infty \phi'_a (2 - \phi'_a) d\zeta \quad (23)$$

$$c = \frac{1}{2} \int_0^\infty (2 - \phi'_a) d\zeta \quad (24)$$

The procedure for obtaining the PA consists in fulfilling local equalities for relations (20) and (21) taking into account the expansion of the exponent (the weight function for the TPPA) at the boundaries of the transition layer. In this case, in the domain of the inner asymptotic ($\zeta \rightarrow 0$), the local equality is written for the expansion in the Taylor series, and

in the domain of the outer asymptotic ($\zeta \rightarrow \infty$), the Loran expansion is used. As a result, the sought solution has the form

$$\phi'_a(\zeta) = 2 \left[1 - \frac{(1 + a_2 D \zeta^3) \exp(-\zeta^2 + c\zeta)}{1 + (a_2 + c)\zeta + \left(a_2^2 + a_2 c + \frac{c^2}{2} - 1\right)\zeta^2 + 2\zeta^4} \right] \quad (25)$$

By solving the system (22)–(24) and using the PA (25), one obtains $a_2 = 0.6641$, $c = 1.7308$, and $D = 0.3357$. The precise numerical solution [51] gives $a_2 = 0.66410$, $c = 1.7208$. Figure 1 shows the graphs for the speed profile $0.5\phi'(\zeta)$.

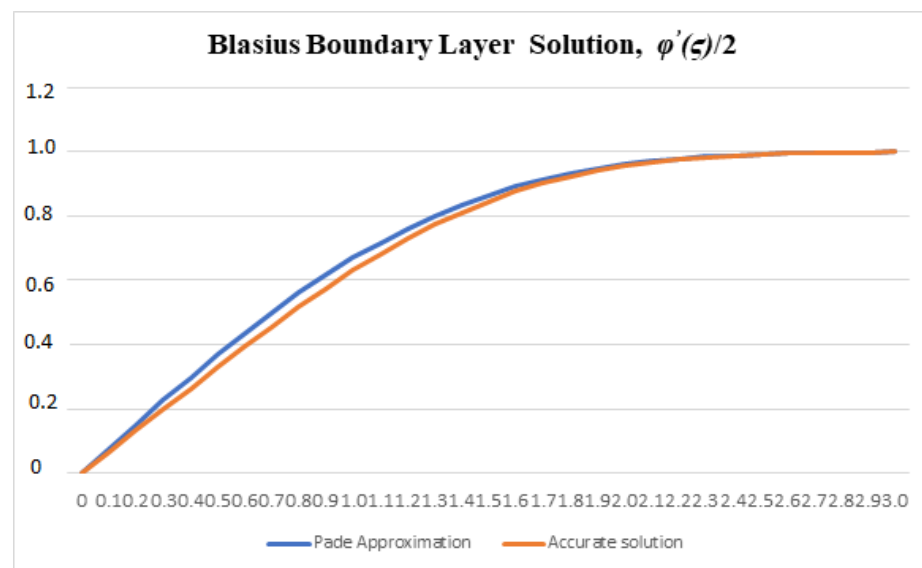


Figure 1. Speed profile for the Blasius boundary layer: the precise numerical solution [51] and the PA.

The function $\frac{1}{2} \frac{d\phi}{d\zeta}$ is a dimensionless value of the velocity profile in the region of the boundary layer of a fluid flowing around a flat plate. This solution is a family of self-similar profiles with affine similarity in all sections of the boundary layer. Thus, if we assume that the velocity at the outer boundary of the layer is constant and equal to U_∞ , then the dimensional value of the velocity has the form $u = U_\infty \frac{1}{2} \frac{d\phi}{d\zeta}$. The maximum error of the PA solution in comparison with the exact solution does not exceed 2%.

7. Application of the PA to the Problem of Rotating Fluid of the Ekman Layer Type

We consider a flow established along the z -axis direction (Figure 2) in a rotating rectangular channel with a side ratio of the order of unity. The distribution of the longitudinal component of the velocity is inhomogeneous along the transverse direction x ; therefore, the influence of the convective terms cannot be neglected. However, at a high speed of rotation, the flow is still divided into a core and thin shear layers such as the Ekman layer on surfaces perpendicular to the axis of rotation [59]. In this case, in contrast to the slotted channel, the layers develop under conditions of an inhomogeneous external flow with a velocity shift in the transverse direction.

Problems of this type are considered in papers [60–67]. Papers [63,64] use the standard reception of decomposition of the sought functions into Fourier series with the further determination of parameters of decompositions by the method of successive approximations. This technique allows us to determine with sufficient accuracy the average characteristics of the flow in the channels. Numerical methods for the solution were used in works [61,62] and [65–67]. It should be noted that in order to correctly apply numerical methods, it is

necessary to take into account the region of singularity of flow near the walls of the channel. In practice, this means that the finite difference grid (or cells in the finite element method) in these regions must be sufficiently shallow (thickened). The thickening methods can be determined analytically or a priori from the flow structure. Methods for such numerical solutions are considered, for example, in works [68,69]. The most stringent of these is *Direct Numerical Simulation (DNS)*. This refers to the numerical integration of three-dimensional non-stationary Navier–Stokes equations on grids, which provide the resolution of all vortex flow structures with minimum scale dimensions. Thus, the DNS method is based on the basic principles of hydro-aerodynamics and is free from empiricism. However, this approach requires a lot of machine time and, given the nonlinear nature of the equations, it is extremely difficult to use parallel algorithms. The second-strictest approach is the so-called *Large-Eddy Simulation (LES)* method, first proposed in Smagorinsky’s work [70]. Within the framework of this method, not the original, but prefiltered Navier–Stokes equations are solved. As a result, using *LES*, only the main “energy-carrying” or “large” vortices are accurately resolved, the sizes of which depend on the size of the filter (its role is usually played by the computational grid used), and smaller vortex structures are approximately modeled using semi-empirical models. Finally, the third relatively new class of approaches, *Hybrid RANS–LES Methods (HRLMs)*, includes a large group of methods that use one or another combination of *RANS* and *LES* methods.

The application of these methods in the calculation of internal currents in rotating channels requires experience with special and expensive application packages. The main difficulty of using numerical methods taking into account the problem of isolating the thin boundary layer area is the lack of a priori information about the structure of the calculation area. In this case, the method we propose can be used to evaluate the geometric parameters of the region. To characterize the thickness of the Ekman boundary layer, you can use the value δ_1 defined by the $|\bar{w} - 1| \leq 0.01$ condition and the value δ_2 equal to the distance from the wall to the point where the velocity component \bar{u} changes the sign to the opposite. By selecting the size of the area of the boundary layer $\delta \sim \max\{\delta_1, \delta_2\}$, this can be used as a priori information to form an uneven grid of the calculated area.

The main characteristic of the inhomogeneity is the local value of the first derivative of the velocity $\frac{dW}{dx}$ in the core along the transverse direction.

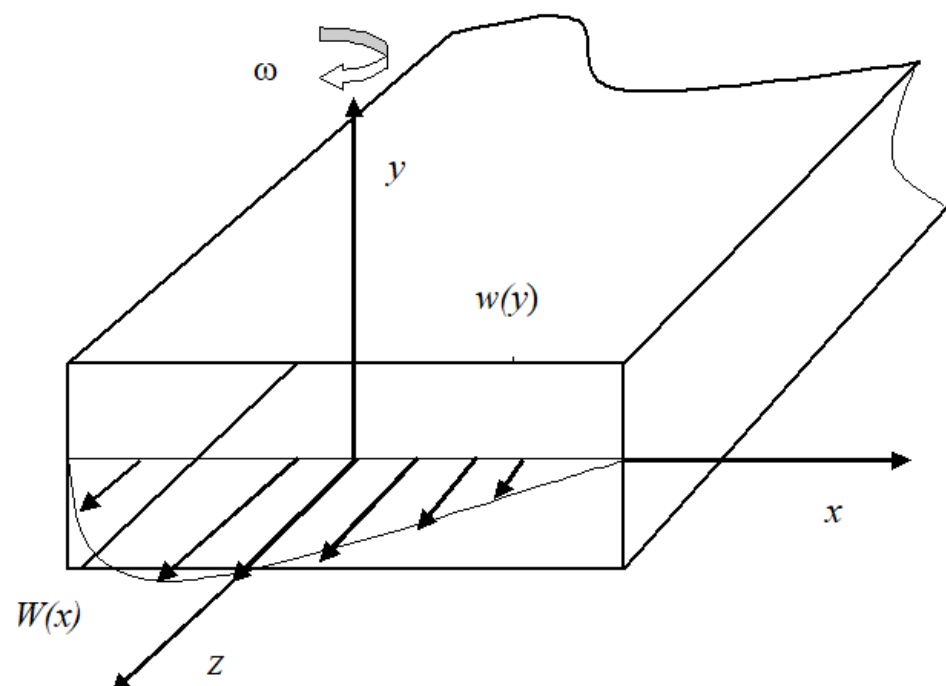


Figure 2. Diagram of flow in a rotating channel.

We deal with a stationary problem and suppose stabilization of flow in the direction of the axis Oz . The equations of motion in a rotating coordinate system are

$$\frac{\partial u}{\partial x} + \frac{\partial v}{\partial y} = 0 \tag{26}$$

$$u \frac{\partial u}{\partial x} + v \frac{\partial u}{\partial y} = -\frac{\partial P^*}{\partial x} - 2\omega w + v \left(\frac{\partial^2 u}{\partial x^2} + \frac{\partial^2 u}{\partial y^2} \right) \tag{27}$$

$$u \frac{\partial w}{\partial x} + v \frac{\partial w}{\partial y} = -\frac{\partial P^*}{\partial x} + 2\omega u + v \left(\frac{\partial^2 w}{\partial x^2} + \frac{\partial^2 w}{\partial y^2} \right) \tag{28}$$

Let us introduce the stream function $\psi(x, y)$

$$\frac{\partial \psi}{\partial x} = -v; \quad \frac{\partial \psi}{\partial y} = u.$$

In accordance with Prandtl's theorem [59], the influence of rotation leads to the equalization of the flow characteristics in the direction of the axis of rotation. Strong viscosity-based rotational effects contribute to the formation of thin (relative to the flow region in the channel) Ekman boundary layers. Following the basic concept of boundary layer theory [50,51], we accept the following assumptions regarding the diffusion of velocity components within the Ekman layer:

$$\frac{\partial^3 \psi}{\partial x^3} \ll \frac{\partial^3 \psi}{\partial y^3}; \quad \frac{\partial^2 w}{\partial x^2} \ll \frac{\partial^2 w}{\partial y^2}.$$

This assumption is based on the analysis of the dimensionality of the specified values for the boundary layer on a flat surface.

Rejecting the terms $\frac{\partial^3 \psi}{\partial x^3}, \frac{\partial^2 w}{\partial x^2}$, we rewrite system (26) and (27) in the form

$$\frac{\partial \psi}{\partial y} \frac{\partial^2 \psi}{\partial x \partial y} - \frac{\partial \psi}{\partial x} \frac{\partial^2 \psi}{\partial y^2} = -\frac{\partial P^*}{\partial x} - 2\omega w + v \left(\frac{\partial^3 \psi}{\partial y^3} \right) \tag{29}$$

$$\frac{\partial \psi}{\partial y} \frac{\partial w}{\partial x} - \frac{\partial \psi}{\partial x} \frac{\partial w}{\partial y} = -\frac{\partial P^*}{\partial x} + 2\omega \frac{\partial \psi}{\partial y} + v \left(\frac{\partial^2 w}{\partial y^2} \right) \tag{30}$$

On the wall we suppose adhesion conditions

$$\begin{aligned} y = -h : w = 0; \quad \frac{\partial \psi}{\partial x} = 0; \quad \frac{\partial \psi}{\partial y} = 0; \\ y = h : w = 0; \quad \frac{\partial \psi}{\partial x} = 0; \quad \frac{\partial \psi}{\partial y} = 0. \end{aligned} \tag{31}$$

We choose the channel half-height h and the local velocity in the median plane $W(x)$ as the length and velocity scales in the section $x = const$. We also introduce the h dimensionless quantities

$$\begin{aligned} \eta = \frac{y}{h}; \quad \bar{w} = \frac{w}{W(x)}; \quad \bar{u} = \frac{u}{W(x)}; \quad \Phi = \frac{\psi}{W(x)h}; \\ Y_0 = \frac{\partial P^+}{\partial x} \frac{h^2}{\nu W(x)}; \quad Z_0 = \frac{\partial P^+}{\partial z} \frac{h^2}{\nu W(x)}; \quad P^* = P - \frac{1}{2} \rho \omega^2 (x^2 + y^2) \end{aligned}$$

Here, P^* is the modified pressure, ω is the angular velocity of rotation, ν is the coefficient of kinematic viscosity, and ρ is the density.

We introduce two dimensionless complexes $Re_\omega = \frac{h^2\omega}{\nu}$ and $Re_c = \frac{hW}{\nu}$. Here, the Reynolds number of rotation Re_ω is a criterion for the similarity of the problem, and parameter Re_c represents the “local number” of Reynolds, depending on the coordinate x . Let us further put $f = \frac{1}{2\omega} \frac{dW}{dx}$, where the value $f = const$ characterizes the “skewness” of the flow in the median plane $y = 0$. It is a local parameter of the inhomogeneity of the external (with respect to the Ekman layer) flow. Let us pass from the variable x to the quantity Re_c , taking the latter as the independent variable. Then

$$\frac{\partial}{\partial x} = \frac{\partial}{\partial Re_c} \frac{dRe_c}{dx} = 2f Re_\omega \frac{\partial}{\partial Re_c}$$

Taking this transformation into account, we write down the equations of motion in dimensionless variables

$$2Re_\omega \left[f \left(\Phi \frac{\partial \bar{w}}{\partial \eta} - \bar{w} \frac{\partial \Phi}{\partial \eta} \right) + \frac{\partial \Phi}{\partial \eta} \right] + \frac{\partial^2 \bar{w}}{\partial \eta^2} - Z_0 = 2f Re_\omega Re_c \left(\frac{\partial \bar{w}}{\partial Re_c} \frac{\partial \Phi}{\partial \eta} - \frac{\partial \Phi}{\partial Re_c} \frac{\partial \bar{w}}{\partial \eta} \right); \quad (32)$$

$$2Re_\omega \left\{ f \left[\Phi \frac{\partial^2 \Phi}{\partial \eta^2} - \left(\frac{\partial \Phi}{\partial \eta} \right)^2 \right] - \bar{w} \right\} + \frac{\partial^2 \bar{w}}{\partial \eta^2} - Y_0 = 2f Re_\omega Re_c \left(\frac{\partial}{\partial Re_c} \left(\frac{\partial \Phi}{\partial \eta} \right) \frac{\partial \Phi}{\partial \eta} - \frac{\partial \Phi}{\partial Re_c} \frac{\partial^2 \Phi}{\partial \eta^2} \right). \quad (33)$$

Equations (32) and (33) contain the quantities f (the parameter of the transverse shear) and Re_c (the parameter of the inhomogeneity of the flow characteristics in the transverse direction). It is known [60] that in channels of rectangular cross-section with the aspect ratio $\kappa = O(1)$, there is a sufficiently long section in the transverse direction, where the parameter $f = const$, that is, the slope of the velocity W_c , is constant and occupies most of the median plane in the plan (see Figure 2).

In our examples, parameter f takes the values $f = 0.95$ near the left wall (the pressure side) and $f = -1.5$ near the right wall (the vacuum side) (shown in Figure 2). Fundamentally, the choice of parameter f is due to a change in the velocity W_c in the flow core: if the velocity W_c increases, then $f > 0$; if W_c decreases, then $f < 0$. The choice of parameter f in our example was made on the basis of speed measurement data in the rotating channel [60].

In this domain, the dependence of the flow characteristics on the local Reynolds number Re_c is weak. This is a consequence of the fact that, due to the relative thinness of the Ekman layers, the scale of the velocity variation in the transverse direction significantly exceeds the linear scale of the velocity variation along the direction normal to the surface. Therefore, in Equations (32) and (33), the right-hand sides can be neglected. Then, in the local approximation, the inhomogeneity of the external flow is provided by the value characterizing the shear in the transverse direction [61]. It should be noted that a similar situation is observed when modeling the nonlinear Ekman layer in geophysical currents caused by the rotation of the Earth [59]. Then, Equations (32) and (33) can be written as follows

$$\bar{w}'' = Z_0 + 2Re_\omega [f(\Phi \bar{w}' - \bar{w} \bar{u}) + \bar{u}] \quad (34)$$

$$\bar{u}'' = Y_0 + 2Re_\omega [f(\Phi \bar{u}' - \bar{u}^2) - \bar{w}] \quad (35)$$

$$\Phi = \int_0^\eta \bar{u} d\eta \quad (36)$$

The BCs are

$$\begin{aligned} \eta = 0 : \bar{w} = 0; \bar{u} = 0; \\ \eta = 1 : w = 1; \bar{u}' = 0; \bar{w}' = 0. \end{aligned} \tag{37}$$

In what follows, we will consider the channel half-height, counting the coordinate from the lower surface (bottom) of the channel. The presence of side walls of the channel assumes that the liquid flow rate through any section of the channel parallel to $x = const$ is

$$\int_0^2 \bar{u} d\eta = 0 \tag{38}$$

Condition (36) makes it possible to determine the values of Y_0 and Z_0 , which characterize the pressure drop in the longitudinal and transverse directions, respectively. In a homogeneous (in direction) kernel, we obtain from Equation (35)

$$Y_0 = -2Re_\omega \bar{w}(1)$$

Taking into account BC (36), one obtains

$$Y_0 = -2Re_\omega \tag{39}$$

Integrating Equation (34), we obtain

$$2Z_0 = 2Re_\omega \int_0^2 \bar{u} d\eta - 2 \left. \frac{d\bar{w}}{d\eta} \right|_{\eta=0} \Rightarrow Z_0 = \bar{w}' \Big|_{\eta=0} \tag{40}$$

To determine the asymptotics of Equations (34) and (35), we consider the inner and outer regions of the flow. Let us call the domain of the near-wall Ekman layer the inner region: $D^i: \eta \in [0, \eta_-)$, where $\eta_- = O(\delta_E)$, δ_E is the thickness of the Ekman layer, and the core of the flow with a uniform velocity distribution is the outer domain $D^e: \eta \in (\eta_+, 1]$, $\eta_+ = O(1)$. For the asymptotic analysis, we perform the stretching of the coordinate taking into account that the thickness of the Ekman layer has an estimate $\delta_E = O(Re_\omega^{-1/2})$ [61].

Let us introduce a new variable

$$\zeta = \eta \sqrt{Re_\omega} \Leftrightarrow \eta = \frac{\zeta}{\sqrt{Re_\omega}} \tag{41}$$

We transform Equations (34) and (35), omitting the dashes above the dimensionless velocity components

$$\frac{d^2 w}{d\zeta^2} = \frac{\alpha}{\sqrt{Re_\omega}} + 2 \left[f \left(\phi \frac{dw}{d\zeta} - wu \right) - u \right] \tag{42}$$

$$\frac{d^2 u}{d\zeta^2} = -2 + 2 \left[f \left(\phi \frac{du}{d\zeta} - u^2 \right) + w \right] \tag{43}$$

$$\phi = \sqrt{Re_\omega} \Phi = \int_0^\zeta u d\zeta, \alpha = - \left. \frac{dw}{d\zeta} \right|_0 \tag{44}$$

Further, we suppose $Re_{\omega_-} \rightarrow \infty$ and consider the flow formed under the strong influence of rotation on the flow. Then, the system of equations of motion has the form

$$w'' = 2f(\phi w' - wu) - 2u \tag{45}$$

$$u'' = 2f(\phi u' - u^2) - 2(1 - w) \tag{46}$$

with BCs

$$\zeta = 0 : w = u = \phi = 0 \tag{47}$$

$$\zeta \rightarrow \infty : w' = u', w = 1, u \rightarrow 0 \tag{48}$$

The last two conditions in (45) take place in the flow core at $|f| = O(1)$, i.e., for relatively small values of the parameter f , which is a consequence of the smallness of δ_E ($\delta_E = O(Re_\omega^{-1/2}) \Rightarrow \delta_E \ll h$) and also by virtue of (37).

Let us choose the formal asymptotic expansions for the flow characteristics in the Ekman layer. The inner asymptotics in the domain D^i are

$$w = a_0 + a_1\zeta + a_2\zeta^2 + a_3\zeta^3 + a_4\zeta^4 + O(\zeta^5) \tag{49}$$

$$\phi = b_0 + b_1\zeta + b_2\zeta^2 + b_3\zeta^3 + b_4\zeta^4 + b_5\zeta^5 + O(\zeta^6) \tag{50}$$

We substitute the expansions (49) and (50) into Equations (42) and (43), taking into account that from the boundary conditions (44) it follows that $a_0 = b_0 = b_1 = 0$

$$\begin{aligned} &2a_2 + 6a_3\zeta + 12a_4\zeta^2 + 20a_5\zeta^3 = \\ &2f(b_2\zeta^2 + b_3\zeta^3 + b_4\zeta^4 + b_5\zeta^5) (a_1 + 2a_2\zeta + 3a_3\zeta^2 + 4a_4\zeta^3 + 5a_5\zeta^4) - \\ &2f(a_1\zeta + a_2\zeta^2 + a_3\zeta^3 + a_4\zeta^4 + a_5\zeta^5) (2b_2\zeta + 3b_3\zeta^2 + 4b_4\zeta^3 + 5b_5\zeta^4) - \\ &2(2b_2\zeta + 3b_3\zeta^2 + 4b_4\zeta^3 + 5b_5\zeta^4) \\ &6b_3 + 24b_4\zeta + 60b_5\zeta^2 = \\ &-2 + 2f(b_2\zeta^2 + b_3\zeta^3 + b_4\zeta^4 + b_5\zeta^5) (2b_2 + 6b_3\zeta + 12b_4\zeta^2 + 20b_5\zeta^3 + 5b_6\zeta^4) - \\ &2f(2b_2\zeta + 3b_3\zeta^2 + 4b_4\zeta^3 + 5b_5\zeta^4)^2 + 2(a_1\zeta + a_2\zeta^2 + a_3\zeta^3 + a_4\zeta^4 + a_5\zeta^5) \end{aligned}$$

Equating the coefficients at the same degrees ζ , we obtain a system for determining the parameters of the expansions (49) and (50)

$$a_2 = 0; 3a_3 = 2b_2; 6a_4 = -fa_1b_2; 5a_5 = -fa_1b_3 - 2b_4; b_3 = -\frac{1}{3}; b_4 = \frac{a_1}{12}; 15b_5 = -fb_2^2 \tag{51}$$

From this system, one obtains

$$a_3 = -\frac{2b_2}{3}; a_4 = -\frac{fa_1}{15} - \frac{a_1}{30}; b_3 = -\frac{1}{3}; b_4 = \frac{a_1}{12}; b_5 = -\frac{fb_2^2}{15}$$

To determine the parameters a_1, b_2 , we use the integral relations [39]. Integrating Equations (42) and (43) with weight 1, we obtain

$$\begin{aligned} &\int_0^\infty w'' d\zeta = 2f \int_0^\infty \phi w' d\zeta - 2f \int_0^\infty w u d\zeta - 2 \int_0^\infty u d\zeta \Rightarrow \\ w' \Big|_0^\infty &= 2f \left[\left| \begin{array}{l} \phi = t, \\ w' d\zeta = dv, \end{array} \right. \begin{array}{l} dt = d\phi \\ v = w \end{array} \right| \phi w \Big|_0^\infty - \int_0^\infty w d\phi \Big] - 2f \int_0^\infty w u d\zeta \Rightarrow \\ &a_1 = 4f \int_0^\infty w u d\zeta; \end{aligned} \tag{52}$$

$$\int_0^\infty u'' d\zeta = 2f \int_0^\infty \phi u' d\zeta - 2f \int_0^\infty u^2 d\zeta - 2 \int_0^\infty (1-w) d\zeta \Rightarrow$$

$$u' \Big|_0^\infty = 2f \left[\left| \begin{matrix} \phi = t, & dt = d\phi \\ du = dv, & v = u \end{matrix} \right| \phi u \Big|_0^\infty - \int_0^\infty u d\phi \right] - 2f \int_0^\infty u^2 d\zeta - 2 \int_0^\infty (1-w) d\zeta \Rightarrow$$

$$b_2 = 2f \int_0^\infty u^2 d\zeta + \int_0^\infty (1-w) d\zeta$$

The inner asymptotics for the velocity components depend on f and have the form

$$w = a_1 \zeta - \frac{2}{3} b_2 \zeta^3 - \frac{f}{6} a_1 b_2 \zeta^4 - \left(\frac{f a_1}{15} + \frac{a_1}{30} \right) \zeta^5 + O(\zeta^6);$$

$$u = 2b_2 \zeta - \zeta^2 + \frac{a_1}{3} \zeta^3 + \frac{f b_2^2}{3} \zeta^4 + O(\zeta^5)$$

Thus, for $f = 0.95$, the inner asymptotics have the form

$$w = a_1 \zeta^2 - \frac{2}{3} b_2 \zeta^3 - \frac{0.95 a_1 b_2}{6} \zeta^4 - \frac{2.19 a_1}{30} \zeta^5 + O(\zeta^6);$$

$$u = 2b_2 \zeta^2 - \frac{1}{3} \zeta^3 + \frac{a_1}{12} \zeta^4 - \frac{0.95 b_2^2}{15} \zeta^5 + O(\zeta^6)$$

Note that at $f = 0.95$, the pressure side (the vertical channel wall) experiences the greatest influence of the secondary flow u . In addition, the choice of $f = 0.95$ is due to the experimental data [60,62].

The outer asymptotics are sought in the form

$$u = B(\zeta) \exp(-\zeta), \quad w = 1 - A(\zeta) \exp(-\zeta)$$

Function $B(\zeta)$ satisfies the fourth-order ODE

$$B^{IV} - 4B^{III} + 6B^{II} - 4B^I + 5B + 4fB = 0$$

For function $A(\zeta)$, one obtains

$$A = -(B'' - 2B' + B) / 2$$

At $f = 0.95$, one obtains:

$$B = -1.69 \exp(-0.19\zeta), \quad A = \exp(-0.19\zeta),$$

$$u \sim -1.19 \exp(-0.19\zeta),$$

$$w \sim 1 - \exp(-0.19\zeta)$$

The PA in the general case can be written as follows

$$w_a = 1 - \frac{1 + \alpha_1 \zeta + \alpha_2 \zeta^2 + \alpha_3 \zeta^3}{1 + \beta_1 \zeta + \beta_2 \zeta^2 + \beta_3 \zeta^3 + \beta_4 \zeta^4} \exp(-\zeta) A(\zeta, f);$$

$$u_a = \frac{\gamma_0 + \gamma_1 \zeta + \gamma_2 \zeta^2}{1 + \delta_1 \zeta + \delta_2 \zeta^2 + \delta_3 \zeta^3} \exp(-\zeta) B(\zeta, f)$$

Specific forms (57) are obtained for given values of f . Consider the PA at $f = 0.95$:

$$w_a = 1 - \frac{1 + \alpha_1 \zeta + \alpha_2 \zeta^2 + \alpha_3 \zeta^3}{1 + \beta_1 \zeta + \beta_2 \zeta^2 + \beta_3 \zeta^3 + \beta_4 \zeta^4} \exp(-1.19\zeta)$$

Comparing the PA (59) and asymptotics (55) and (56), one obtains

$$\alpha_1 = \beta_1 + 1.19 - a_1; \alpha_2 = \frac{\frac{2}{3}b_2 - (1.43 + a_1^2)\beta_1 - 1.70}{a_1 - 1.19}$$

$$\alpha_3 = \frac{1.13b_2 - 2.43\beta_1 - 2.87}{a_1} - \frac{1.97}{a_1 - 1.19} + \frac{1.13b_2 - 2.43\beta_1 - 3.45}{a_1(a_1 - 1.19)}$$

$$\beta_1 = \frac{c}{d}$$

where:

$$c = \frac{0.72 - 3a_1}{a_1 - 1.19} + \frac{2b_2 - 5.10}{a_1(a_1 - 1.19)} + \frac{1.69b_2 - 4.29}{a_1(a_1 - 1.19)} - \frac{1.80}{b_2(a_1 - 1.19)}$$

$$d = 1 + \frac{1.07a_1^2 + 1.53}{b_2(a_1 - 1.19)} + \frac{4.29}{a_1(a_1 - 1.19)} + \frac{3.57}{a_1} \tag{62}$$

$$\beta_2 = \frac{1.03 - 1.43\beta_1}{a_1} + \frac{0.79b_2 - (1.19a_1^2 + 1.70)\beta_1 - 2.04}{a_1(a_1 - 1.19)}$$

$$\beta_3 = 0; \beta_4 = 0$$

The PA for the velocity component u at $f = 0.95$ can be represented as

$$u_a = \frac{\gamma_0 + \gamma_1\zeta + \gamma_2\zeta^2}{1 + \delta_1\zeta + \delta_2\zeta^2 + \delta_3\zeta^3} 1.69 \exp(-1.19\zeta) \tag{63}$$

Comparing the PA (60) and asymptotics (55) and (58), one obtains

$$\gamma_0 = 0; \gamma_1 = 0; \gamma_2 = -1.18b_2; \delta_1 = \frac{1}{6b_2} - 1.19; \delta_2 = \gamma_2; \delta_3 = 0$$

The PA parameters are expressed using integral ratios similar to the way it is done in [39]

$$a_1 = 2 \int_0^\infty u_a(1 + fw_a)d\zeta - 2f \int_0^\infty \phi_a \cdot w'_a d\zeta \tag{64}$$

$$b_2 = f \int_0^\infty u'_a{}^2 d\zeta - f \int_0^\infty \phi_a \cdot u'_a d\zeta - \int_0^\infty (1 - w)d\zeta \tag{65}$$

Relations (61) and (62) are calculated by numerical integration using quadrature formulas. For $f = 0$, one obtains the well-known Ekman solution [59], which can be found analytically from (42) and (43):

$$w = 1 - \exp(-\zeta) \cos \zeta; u = \exp(-\zeta) \sin \zeta \tag{66}$$

Figure 3 shows the profiles of the dimensionless velocity components $\bar{u} = \frac{u}{u_e}$ and $\bar{w} = \frac{w}{w_e}$ for different values of f . Curves 1 and 2 correspond to $f = 0$, curves 3 and 4 correspond to $f = -1.5$, and curves 5 and 6 correspond to $f = 0.95$. The graphs of the distributions of the velocity components show a tendency towards a decrease in the local maximum of the velocity component w with an increase in the parameter f , up to complete degeneration at $f = 0.95$. In this case, the intensity of the secondary current increases, as evidenced by an increase in the local maximum of the profile u near the wall and an increase in the thickness of the wall layer, in which the liquid is transferred in the transverse direction.

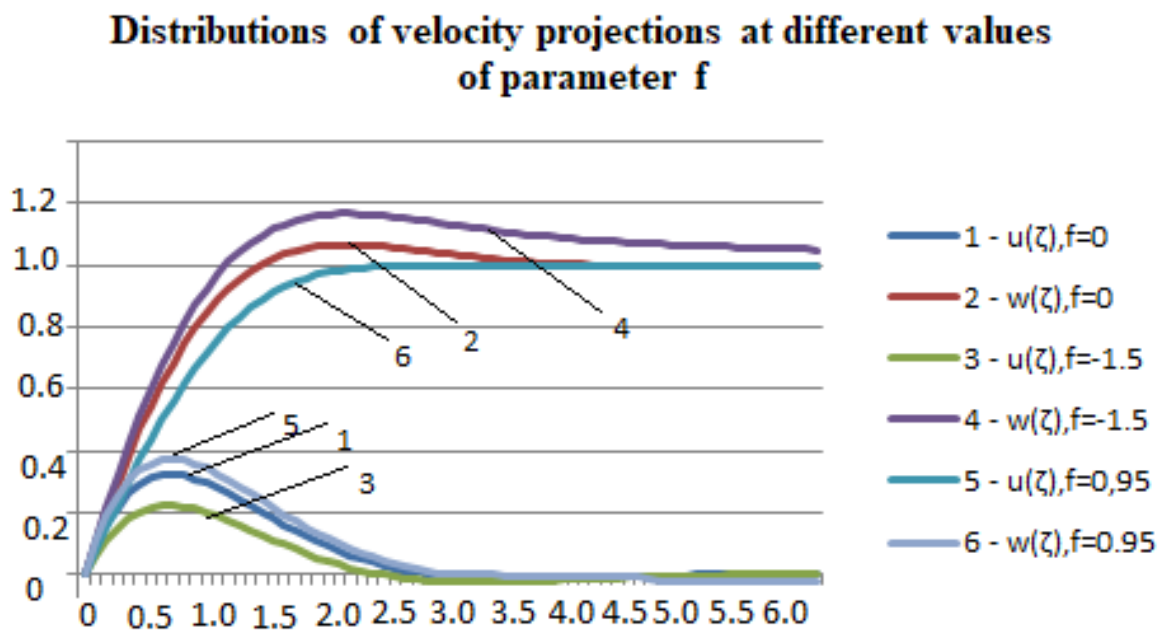


Figure 3. Velocity profile graphs for different parameter f values.

The interest in solving the Ekman boundary layer problem on surfaces perpendicular to the axis of rotation is due to practical applications in more complex problems of calculating internal currents in rotating systems. These may be the regions of fluid flow between the blades of turbogenerators. The results of solving the problem can be used to estimate the intensity of secondary currents in the flow core, as well as to estimate the effects of rotation on the coefficient of resistance. The intensity of the secondary currents is determined by integrating the velocity component $\bar{u} = \frac{u}{u_e}$ across the channel. As can be seen in Figure 3, the profile of this component forms an increasing secondary flow in the region of positive values of the parameter $f = \frac{1}{\omega} \frac{dW_c}{dx}$. In this case, the secondary flow velocity profile $\bar{u} = \frac{u}{u_e}$ changes its sign at a distance from the horizontal surface of the channel. Thus, vortex structures are formed in the transverse plane of the channel under the action of secondary flow. The role of secondary flow intensity is important from the point of view of assessing its effect on the flow rate of liquid circulating in the direction of the Ox axis. Works [60–63] note the determining contribution of the Ekman layer to the resistance (surface friction) of the channel with radial flow of the liquid. The channel resistance coefficient increases as the rotation parameter $Re_\omega = \frac{h^2\omega}{\nu}$ increases. The decisive contribution of the Ekman layer to the total amount of superficial friction depends also on a distinction between the geometrical forms of the cross-section of the channel: with the growth of parameter $\kappa = \frac{l}{2h}$, where l is the length of a horizontal lower wall of the channel, h (half of the height of the channel) increases the resistance coefficient.

With an increase in the absolute value of $|f|$, at $f < 0$, the local maximum of the velocity component w near the wall is more pronounced, and the intensity of the secondary flow (the velocity component u) decreases. The tendencies noted are fully consistent with those observed in the laminar nonlinear Ekman layer [59,62] and are in qualitative agreement with the experimental data [60].

8. Conclusions

The main part of our paper discusses using the PA for problems of incompressible fluid mechanics. Attention is drawn to the fact that this approach is the most effective for the problems of boundary layer theory. Considering the problems of streamlining

bodies in the external and internal currents of a viscous fluid, we focus on transition layers. Transient layers are regions of disjoint asymptotic decomposition occurring in the vicinity of boundaries where unevenness is due to the physical essence of the phenomenon as well as the joint interaction of several factors determined through external parameters. At the same time, if localization is achieved using asymptotics, then the description of the transition region or transition layer is carried out using a PA.

The main advantages of using a PA are:

- the possibility of taking into account the peculiarities of the desired solution and describing non-trivial behavior in the vicinity of internal and external boundaries;
- the representation of the interpolated solution by an analytical expression; and
- the possibility of subsequent mathematical analysis of the obtained analytical expressions in the form of a PA (differentiation, integration, construction of functionals, etc.)

The essence of the proposed calculation technique is that internal and external asymptotics acting in different areas are not stitched together a priori at an unknown point or in an unknown area but are connected by a continuous dependence. The natural problems of hydrodynamics provide rich material for theoretical generalizations and significant advances in the field of asymptotic mathematics. Analyzing the methodological features of the method, we consider the known problems for the Blasius boundary layer and the Ekman boundary layer in rotating channels. These problems have known numerical solutions. This makes it possible to compare the decisions we have made. The accuracy of the solutions obtained using asymptotic methods and the subsequent interpolation of PA solutions is quite satisfactory. As noted above, the solutions we have obtained have an analytical appearance, which gives great advantages in the subsequent analysis of solutions. Furthermore, the obvious ease of obtaining solutions is a significant factor. This is especially evident in solving the Blasius self-similar problem. Solving the Ekman problem in a rotating channel is not a self-similar problem; however, using parameterization with a quantity $f = \frac{1}{\omega} \frac{dW_c}{dx}$, we obtain a sequence of self-similar tasks at given values of parameter f .

Author Contributions: Conceptualization, I.A.; methodology, I.A. and A.S.; investigation, I.A. and A.S.; writing—original draft preparation, I.A.; formal analysis, A.S. All authors have read and agreed to the published version of the manuscript.

Funding: This research received no external funding.

Institutional Review Board Statement: Not applicable.

Informed Consent Statement: Not applicable.

Data Availability Statement: Data are contained within the article.

Acknowledgments: The authors thank Galina A. Starushenko for valuable discussions.

Conflicts of Interest: The authors declare that they have no conflict of interest.

References

1. Boyd, J.P. Padé approximant algorithm for solving nonlinear ordinary differential equation boundary value problems on an unbounded domain. *Comput. Phys.* **1997**, *11*, 299–303. [[CrossRef](#)]
2. Andrianov, I.V.; Awrejcewicz, J. New trends in asymptotic approaches: Summation and interpolation methods. *Appl. Mech. Rev.* **2001**, *54*, 69–92. [[CrossRef](#)]
3. Andrianov, I.V.; Awrejcewicz, J.; Danishevs'kyi, V.V.; Ivankov, A.O. *Asymptotic Methods in the Theory of Plates with Mixed Boundary Conditions*; John Wiley & Sons: Hoboken, NJ, USA, 2014.
4. Andrianov, I.V.; Awrejcewicz, J.; Danishevs'kyi, V.V. *Linear and Nonlinear Waves in Microstructured Solids: Homogenization and Asymptotic Approaches*; CRC Press Taylor & Francis: Boca Raton, FL, USA, 2021.
5. Apresyan, L.A. Padé approximants. *Radiophys. Quantum Electron.* **1979**, *22*, 449–466. [[CrossRef](#)]
6. Basdevant, J.L. The Padé approximation and its physical applications. *Fortschr. Phys.* **1972**, *20*, 283–328. [[CrossRef](#)]
7. Baker, G.A.; Graves-Morris, P. *Padé Approximants*; Cambridge University Press: Cambridge, UK, 1996.
8. Gonnet, P.; Güttel, S.; Trefethen, L.N. Robust Padé approximation via SVD. *SIAM Rev.* **2013**, *55*, 101–117. [[CrossRef](#)]

9. Jones, W.B.; Thron, W.J. *Continued Fractions: Analytic Theory and Applications*; Addison-Wesley: Reading, MA, USA, 1980.
10. Boyd, J.P. The Devil's invention: Asymptotic, superasymptotic and hyperasymptotic series. *Acta Appl. Math.* **1999**, *56*, 1–98. [[CrossRef](#)]
11. Brezinski, C. Convergence acceleration during the 20th century. *J. Comput. Appl. Math.* **2000**, *122*, 1–21. [[CrossRef](#)]
12. Suetin, S.P. Padé approximants and efficient analytic continuation of a power series. *Russ. Math. Surv.* **2002**, *57*, 43–141. [[CrossRef](#)]
13. Vyatchin, A.V. On convergence of Padé approximants. *Moscow Univ. Math. Bull.* **1982**, *37*, 1–4.
14. Smith, D.A.; Ford, W.F. Acceleration of linear and logarithmic convergence. *SIAM J. Numer. Anal.* **1979**, *16*, 223–240. [[CrossRef](#)]
15. Holub, A.P. Method of generalized moment representations in the theory of rational approximation (a survey). *Ukr. Math. J.* **2003**, *55*, 377–433. [[CrossRef](#)]
16. Litvinov, G.L. Approximate construction of rational approximations and the effect of autocorrection error. *Russ. J. Math. Phys.* **1993**, *1*, 313–352.
17. Litvinov, G.L. Error autocorrection in rational approximation and interval estimation. [A survey of results.]. *Centr. Eur. J. Math.* **2003**, *1*, 36–60.
18. Luke, Y.L. Computations of coefficients in the polynomials of Padé approximants by solving systems of linear equations. *J. Comp. Appl. Math.* **1980**, *6*, 213–218. [[CrossRef](#)]
19. Luke, Y.L. A note on evaluation of coefficients in the polynomials of Padé approximants by solving systems of linear equations. *J. Comp. Appl. Math.* **1982**, *8*, 93–99. [[CrossRef](#)]
20. Gilewicz, J.; Pindor, M. Padé approximants and noise: Rational a case of geometrical series. *J. Comp. Appl. Math.* **1997**, *87*, 199–214. [[CrossRef](#)]
21. Gilewicz, J.; Pindor, M. Padé approximants and noise: Rational functions. *J. Comp. Appl. Math.* **1999**, *105*, 285–297. [[CrossRef](#)]
22. Beckermann, B.; Kaliaguine, V. The diagonal of the Padé table and the approximation of the Weyl function of the second-order difference operator. *Constr. Approx.* **1997**, *13*, 481–510. [[CrossRef](#)]
23. Schött, J.; Loch, I.L.M.; Lundin, E.; Grånäs, O.; Eriksson, O.; Di Marco, I. Analytic continuation by averaging Padé approximants. *Phys. Rev. B* **2016**, *93*, 075104. [[CrossRef](#)]
24. Badikov, S.A.; Vinogradov, V.A.; Gai, E.V.; Rabotnov, N.S. Analytic approximation of neutron physics data. *Sov. At. Energy* **1984**, *56*, 19–26. [[CrossRef](#)]
25. Frost, P.A.; Harper, E.Y. Extended Padé procedure for constructing global approximations from asymptotic expansions: An explication with examples. *SIAM Rev.* **1976**, *18*, 62–91. [[CrossRef](#)]
26. Martin, P.; Baker, G.A., Jr. Two-point quasifractional approximant in physics. Truncation error. *J. Math. Phys.* **1991**, *32*, 1470–1477. [[CrossRef](#)]
27. Drazin, P.G.; Tourigny, Y. Numerical study of bifurcations by analytic continuation of a function defined by a power series. *SIAM J. Appl. Math.* **1996**, *56*, 1–18. [[CrossRef](#)]
28. Gluzman, S.; Mityushev, V.; Nawalaniec, W. *Computational Analysis of Structured Media*; Elsevier: Amsterdam, The Netherlands, 2017.
29. Zemlyanukhin, A.I.; Bochkarev, A.V. Perturbation method and exact solutions of equations of nonlinear dynamics of media with microstructure. *Comput. Cont. Mech.* **2016**, *9*, 182–191. (In Russian) [[CrossRef](#)]
30. Bochkarev, A.V.; Zemlyanukhin, A.I. The geometric series method for constructing exact solutions to nonlinear evolution equations. *Comput. Math. Math. Phys.* **2017**, *57*, 1111–1123. [[CrossRef](#)]
31. Andrianov, I.; Zemlyanukhin, A.; Bochkarev, A.; Erofeev, V. Steady solitary and periodic waves in nonlinear nonintegrable lattice. *Symmetry* **2020**, *12*, 1608. [[CrossRef](#)]
32. Boyd, J. Strongly nonlinear perturbation theory for solitary waves and bions. *Evol. Equ. Control Theory* **2019**, *8*, 1–29. [[CrossRef](#)]
33. Barlow, N.S.; Stanton, C.R.; Hill, N.; Weinstein, S.J.; Cio, A.G. On the summation of divergent, truncated, and underspecified power series via asymptotic approximants. *Q. J. Mech. Appl. Math.* **2017**, *70*, 21–48. [[CrossRef](#)]
34. Van Dyke, M. Computer extension of perturbation series in fluid mechanics. *SIAM J. Appl. Math.* **1975**, *28*, 720–734. [[CrossRef](#)]
35. Van Dyke, M. From zero to infinite R by computing extension of Stokes series. In *Singular Perturbations and Boundary Layer Theory*; Springer: Berlin/Heidelberg, Germany, 1977; Volume 594, pp. 506–517.
36. Van Dyke, M. Analysis and improvement of perturbation series. *Q. J. Mech. Appl. Math.* **1974**, *27*, 423–450. [[CrossRef](#)]
37. Pozzi, A. *Application of Padé Approximation Theory in Fluid Dynamics*; World Scientific: Singapore, 1994.
38. Shatrov, A.V. Method of matching of interior and exterior asymptotics in boundary-value problems of mathematical physics. *J. Math. Sci.* **2018**, *230*, 804–807. [[CrossRef](#)]
39. Andrianov, I.; Shatrov, A. Padé approximation to solve the problems of aerodynamics and heat transfer in the boundary layer. In *Mathematical Theorems*; IntechOpen: London, UK, 2020.
40. Tropp, E.A. The idea of boundary layer beyond Prandtl theory. In *Problems of Fluid and Gas Mechanics*; SPb, SPb State University: Sankt-Petersburg, Russia, 2000; pp. 125–133.
41. Van Dyke, M. Nineteenth-century roots of the boundary-layer idea. *SIAM Rev.* **1994**, *36*, 415–424. [[CrossRef](#)]
42. Malley, R.E. *Historical Developments in Singular Perturbations*; Springer: New York City, NY, USA, 2014.
43. Calladine, C.R. The theory of thin shell structures 1888–1988. In *Proceedings of the Institution of Mechanical Engineers, Part A: Power and Process Engineering*; SAGE Publications: London, UK, 1988; Volume 202, pp. 141–149.
44. Van Dyke, M. *An Album of Fluid Motion*; The Parabolic Press: Stanford, CA, USA, 1982.

45. Vishik, M.I.; Lyusternik, L.A. Regular degeneration and boundary layer for linear differential equations with small parameters. *Amer. Math. Surv. Transl.* **1962**, *2*, 239–364.
46. Vishik, M.I.; Lyusternik, L.A. The asymptotic behaviour of solutions of linear differential equations with large or quickly changing coefficients and boundary conditions. *Russ. Math. Surv.* **1960**, *15*, 23–91. [[CrossRef](#)]
47. Višik, M.I.; Lyusternik, L.A. Initial jump for nonlinear differential equations containing a small parameter. *Soviet Math. Dokl.* **1960**, *1*, 749–752.
48. Nayfeh, A. *Introduction to Perturbation Techniques*; John Wiley & Sons: New York, NY, USA, 1981.
49. Barantsev, R.G. Asymptotic versus classical mathematics. *Top. Math. Anal.* **1989**, 49–64. [[CrossRef](#)]
50. Loitsyanskii, L.G. *Laminar Boundary Layer*; For. Techn. Div. Wright-Patterson AFB: Greene County, OH, USA, 1964.
51. Loitsyanskii, L.G. *Mechanics of Liquids and Gases*; Pergamon Press: Elmsford, NY, USA, 1966.
52. Roache, P.J. *Computation Fluid Dynamics*; Hermosa Publishers: Albuquerque, NM, USA, 1976.
53. Lapin, Y.V. Development of the theory of the boundary layer in the USSR for 70 years (1917–1987). In *Problems of Fluid and Gas Mechanics*; SPb, SPbSTU: Sankt-Petersburg, Russia, 2000; pp. 73–113.
54. Van Dyke, M. *Perturbation Methods in Fluid Mechanics*; The Parabolic Press: Stanford, CA, USA, 1975.
55. Kevorkian, J.; Cole, J.D. *Perturbation Methods in Applied Mathematics*; Springer: New York City, NY, USA, 1981.
56. Barantsev, R.G.; Engelgart, V.N. *Asymptotic Methods in Gas and Fluid Dynamics*; LSU: Leningrad, Russia, 1987. (In Russian)
57. Eckhaus, W. *Asymptotic Analysis of Singular Perturbations*; North Holland: Amsterdam, The Netherlands, 1979.
58. Il'in, A.M. *Matching of Asymptotic Expansions of Solutions of Boundary Value Problems*; AMS: Providence, RI, USA, 1992.
59. Greenspan, H.P. *The Theory of Rotating Fluids*; Cambridge University Press: Cambridge, UK, 1968.
60. Smirnov, E.M.; Yurkin, S.V. Fluid flow in a rotating channel of square section. *Fluid Dyn.* **1983**, *18*, 850–855. [[CrossRef](#)]
61. Smirnov, E.M.; Shatrov, A.V. Modeling strong effects of rotating system in computation of turbulent flows in channels. *J. Appl. Mech. Tech. Phys.* **1985**, *26*, 635–640. [[CrossRef](#)]
62. Smirnov, E.M. Local breakdown of the two-eddy secondary flow structure in a rotating channel for small and large inlet nonuniformities. *Fluid Dyn.* **1999**, *34*, 333–341.
63. Ovchinnikov, O.N. Steady flow of viscous fluid through a rotating radial channel at small values of the Rossby numbers. *J. Appl. Mech. Tech. Phys.* **1980**, *25*, 76–83.
64. Sergeev, S.I. Flow in rotating radial channels at small Rossby and Ekman numbers. *Fluid Dyn.* **1984**, *19*, 8–12. [[CrossRef](#)]
65. Julien, S.; Torriano, F.; Dumas, G.; Maciel, Y. Investigation of the 3D inlet flow characteristics in a rotating channel setup. *Can. Congr. Appl. Mech.* **2005**, 521–572.
66. Julien, S.; Dumas, G.; Torriano, F.; Maciel, Y. Secondary flow and roll cells interaction in high-aspect-ratio rotating turbulent duct flows. *Int. J. Comput. Fluid Dyn.* **2008**, *22*, 19–28. [[CrossRef](#)]
67. Torriano, F.; Stella, S.; Jayet, Y.; Ardaillon, T.; Charest-Fournier, J.-P.; Hudon, C.; Merkhouf, A.; Guillot, A. Numerical and experimental study of the ventilation in an operating hydrogenerator. In *AIP Conference Proceedings*; AIP Publishing LLC: Melville, NY, USA, 2019; Volume 2116, p. 450003.
68. Hirsch, C. *Numerical Computation of Internal and External Flows. Vol. 1 Fundamentals of Computational Fluid Dynamics*, 2nd ed.; Elsevier: Amsterdam, The Netherlands, 2007.
69. Manni, L.; Nishino, T.; Delafin, P.L. Numerical study of airfoil stall cells using a very wide computational domain. *Comput. Fluids* **2016**, *140*, 260–269. [[CrossRef](#)]
70. Smagorinsky, J. General circulation experiments with the primitive equation. I. The basic experiments. *Mon. Weather Rev.* **1963**, *91*, 99–164. [[CrossRef](#)]